

Journal of Digital Imaging
Deep Learning for Brain MRI Segmentation: State of The Art and Future Directions
 --Manuscript Draft--

Manuscript Number:	JDIM-D-17-00060R1	
Full Title:	Deep Learning for Brain MRI Segmentation: State of The Art and Future Directions	
Article Type:	Review	
Funding Information:	National Cancer Institute (U01CA160045)	Dr Bradley J. Erickson
	National Cancer Institute (U01CA142555)	Dr Daniel L. Rubin
Abstract:	<p>Quantitative analysis of brain MRI is routine for many neurological diseases and conditions, and relies on accurate segmentation of structures of interest. Deep learning-based segmentation approaches for brain MRI are gaining interest due to their self-learning and generalization ability over large amounts of data. As the deep learning architectures are becoming more mature, they gradually outperform previous state-of-the-art classical machine learning algorithms. This review aims to provide an overview of current deep learning-based segmentation approaches for quantitative brain MRI. First we review the current deep learning architectures used for segmentation of anatomical brain structures and brain lesions. Next, the performance, speed, and properties of deep learning approaches are summarized and discussed. Finally, we provide a critical assessment of the current state, and identify likely future developments and trends.</p>	
Corresponding Author:	<p>Bradley Erickson, M.D. Ph.D. Mayo Clinic - Rochester Rochester, Minnesota UNITED STATES</p>	
Corresponding Author Secondary Information:		
Corresponding Author's Institution:	Mayo Clinic - Rochester	
Corresponding Author's Secondary Institution:		
First Author:	Zeynettin Akkus, PhD	
First Author Secondary Information:		
Order of Authors:	Zeynettin Akkus, PhD	
	Alfiia Galimzianova, PhD	
	Assaf Hoogi, PhD	
	Daniel L. Rubin, MD	
	Bradley J. Erickson, MD, PhD	
Order of Authors Secondary Information:		
Author Comments:	<p>Dear Editor,</p> <p>We thank the anonymous reviewer for the positive response on our manuscript and the constructive comments. We have revised the manuscript accordingly, and in the following provide point-by-point responses to the comments and corresponding changes to the manuscript.</p> <p>Sincerely, Bradley J Erickson, MD PhD</p>	

[Click here to view linked References](#)1
2
3
4
5
6
7
8
9
10
11
12

Deep Learning for Brain MRI Segmentation: State of The Art and Future Directions

Abstract

Quantitative analysis of brain MRI is routine for many neurological diseases and conditions, and relies on accurate segmentation of structures of interest. Deep learning-based segmentation approaches for brain MRI are gaining interest due to their self-learning and generalization ability over large amounts of data. As the deep learning architectures are becoming more mature, they gradually outperform previous state-of-the-art classical machine learning algorithms. This review aims to provide an overview of current deep learning-based segmentation approaches for quantitative brain MRI. First we review the current deep learning architectures used for segmentation of anatomical brain structures and brain lesions. Next, the performance, speed, and properties of deep learning approaches are summarized and discussed. Finally, we provide a critical assessment of the current state, and identify likely future developments and trends.

Keywords: Deep learning, quantitative brain MRI, convolutional neural network, brain lesion segmentation

24
25
26
27
28
29
30
31
32
33
34
35
36
37
38
39
40
41
42
43
44
45
46
47
48
49
50
51
52
53
54
55
56
57
58
59
60
61
62
63
64
65

1
2
3
4 **1. Background**

5 Magnetic resonance imaging (MRI) is usually the modality of choice for structural brain analysis,
6 since it provides images with high contrast for soft tissues and high spatial resolution, and presents no
7 known health risks. While modalities such as computed tomography (CT) and positron emission
8 tomography (PET) are also used to study the brain, MRI is the most popular, and we will focus on MRI in
9 this work. Quantitative analysis of brain MRI has been used extensively for characterization of brain
10 disorders such as Alzheimer's disease, epilepsy, schizophrenia, multiple sclerosis (MS), cancer, and
11 infectious and degenerative diseases. For example, tissue atrophy is one of the common biomarkers
12 used in diagnosis and therapy assessment in Alzheimer's disease, epilepsy, schizophrenia, MS, and
13 many other neurological diseases and disorders. To quantify tissue atrophy, segmentation and
14 corresponding measurements of brain tissues are needed. Similarly, quantification of change in brain
15 structures requires segmentation of the MRI obtained at different time points. In addition, detection and
16 precise localization of the abnormal tissue and surrounding healthy structures are crucial for diagnosis,
17 surgical planning, postoperative analysis and chemo/radiotherapy planning. Quantitative and qualitative
18 characterization of normal and pathological structures, both in space and time, are often part of clinical
19 trials, in which the effects of treatment are studied on a cohort of patients and normal controls.
20
21

22 Quantitative analysis of brain MR images is routine for many neurological diseases and
23 conditions. Segmentation, i.e., labeling of pixels in 2D (voxels in 3D), is a critical component of
24 quantitative analysis. Manual segmentation is the gold standard for *in vivo* images. However, this requires
25 outlining structures slice-by-slice, and is not only expensive and tedious, but also inaccurate due to
26 human error. Therefore, there is a need for automated segmentation methods to provide accuracy close
27 to that of expert raters' with a high consistency.
28
29

30 As 3D and 4D imaging are becoming routine, and with physiological and functional imaging
31 increasing, medical imaging data is increasing in size and complexity. Therefore, it is essential to develop
32 tools that can assist in extracting information from these large datasets. Machine learning is a set of
33 algorithmic techniques that allow computer systems to make data-driven predictions from large data.
34 These techniques have a variety of applications that can be tailored to the medical field.
35
36

37 There has been a significant effort in developing classical machine learning algorithms for
38 segmentation of normal (e.g. white matter and gray matter) and abnormal brain tissues (e.g. brain tumors)
39 in MRI. However, creation of the imaging features that enable such segmentation requires careful
40 engineering and specific expertise. Furthermore, traditional machine learning algorithms do not
41 generalize well. Despite a significant effort from the medical imaging research community, automated
42 segmentation of the brain structures and detection of the abnormalities remain an unsolved problem due
43 to normal anatomical variations in brain morphology, variations in acquisition settings and MRI scanners,
44 image acquisition imperfections, and variations in the appearance of pathology.
45
46

47 An emerging machine learning technique referred to as deep learning [1], can help avoid
48 limitations of classical machine learning algorithms, and its self-learning of features may enable
49 identification of new useful imaging features for quantitative analysis of brain MRI. Deep learning
50 techniques are gaining popularity in many areas of medical image analysis [2], such as computer-aided
51 detection of breast lesions [3], computer-aided diagnosis of breast lesions and pulmonary nodules [4],
52 and in histopathological diagnosis [5]. In this survey, we provide an overview of state-of-the-art deep
53 learning techniques in the field of brain MR segmentation and discuss remaining gaps that have a
54 potential to be fulfilled by the use of deep learning techniques.
55
56

57 **1.1. Deep Learning**

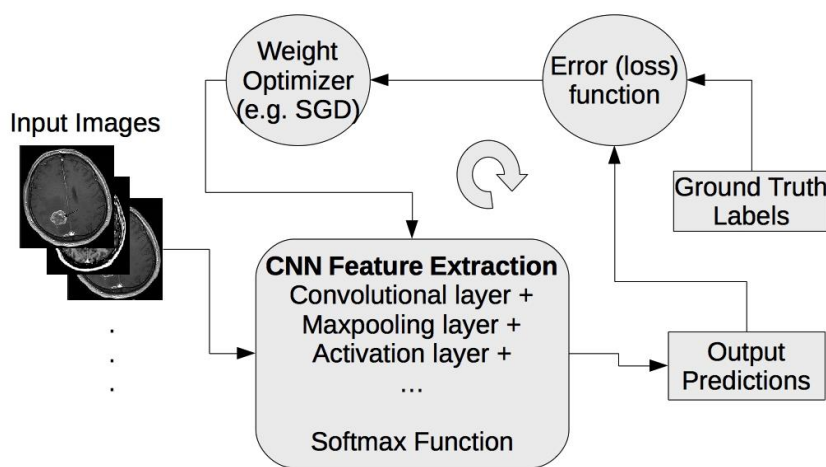
58 Deep Learning refers to neural networks with many layers (usually more than 5) that extract a
59 hierarchy of features from raw input images. It is a new and popular type of machine learning techniques
60 that extract a complex hierarchy of features from images due to their self-learning ability as opposed to
61 the hand-crafted feature extraction in classical machine learning algorithms. They achieve impressive
62
63
64
65

1
2
3
4 results and generalizability by training on large amount of data. The rapid increase in GPU processing
5 power has enabled the development of state-of-the-art deep learning algorithms. This allowed training of
6 deep learning algorithms with millions of images and provided robustness to variations in images.
7

8 There are several types of deep learning approaches that have been developed for different
9 purposes, such as object detection and segmentation in images, speech recognition, and
10 genotype/phenotype detection and classification of diseases. Some of the known deep learning
11 algorithms are stacked auto-encoders, deep Boltzmann machines, deep neural networks, and
12 convolutional neural networks (CNNs). CNNs are the most commonly applied to image segmentation and
13 classification.
14

15 CNNs were first introduced in 1989 [6], but gained great interest after deep CNNs achieved
16 spectacular results in ImageNet [8], [9] competition in 2012 [7]. Applied on a dataset of about a million
17 images that included 1000 different classes, CNNs nearly halved the error rates of the previously best
18 computing approaches [7].
19

20 CNN architectures are increasingly complex, with some systems having more than 100 layers,
21 which means millions of weights and billions of connections between neurons. A typical CNN architecture
22 contains subsequent layers of convolution, pooling, activation, and classification (fully connected).
23 Convolutional layer produces feature maps by convolving a kernel across the input image. Pooling layer
24 is used to downsample the output of preceding convolutional layers by using the maximum or average of
25 the defined neighborhood as the value passed to the next layer. Rectified Linear Unit (ReLU) and its
26 modifications such as Leaky ReLU are among the most commonly used activation functions. ReLU
27 nonlinearly transforms data by clipping any negative input values to zero while positive input values are
28 passed as output [10]. To perform a prediction of an input data, the output scores of the final CNN layer
29 are connected to loss function (e.g. cross-entropy loss that normalizes scores into multinomial distribution
30 over labels). Finally, parameters of the network are found by minimizing a loss function between
31 prediction and ground truth labels with regularization constraints, and the network weights are updated at
32 each iteration (e.g. using stochastic gradient descent – SGD) using backpropagation until convergence
33 (see Figure 1).
34
35



55 Figure 1. A schematic representation of a convolutional neural network (CNN) training process.
56

57 2. Review 58

59 We performed a thorough analysis of the literature using the Google Scholar and NLM Pubmed
60 search engines. We included all found peer reviewed journal publications and conference proceedings
61
62

that describe applying deep learning to brain MRI segmentation. Since a large fraction of deep learning works are submitted to Arxiv (<http://arxiv.org>) first, we also included relevant Arxiv preprints. Conference proceedings that had a follow-up journal publication were included only in their final publication form. We divided papers into two groups: works on normal structures and on brain lesions. In both groups, different deep learning architectures have been introduced to address domain-specific challenges. We further subdivided them based on their architecture style such as patch-wise, semantic-wise, or cascaded architectures. In the following subsections, we present evaluation and validation methods, preprocessing methods used in current deep learning approaches, current deep learning architecture styles, and performance of deep learning algorithms for quantification of brain structures and lesions.

2.1. Training, Validation and Evaluation

In the machine learning field, data are divided into training, validation, and test sets for learning from examples, establishing the soundness of learning results, and evaluating the generalization ability of a developed algorithm on unseen data, respectively. When there are limited data, cross validation methods (e.g. one-leave out, 5-fold, or 10-fold validations) are preferred. In a k-fold cross-validation, the data are randomly partitioned into k equal sized parts. One of the k parts is retained as the validation data for testing the algorithm, and the remaining k – 1 parts are used as training data. Training is typically done with a supervised approach which requires ground truth for the task. Ground truth is usually obtained with manual delineations of brain lesions or structures by experts for segmentation tasks. Even though this is the gold standard for the learning and evaluation, it is a tedious and laborious task and contains subjectivity. In their work, Mazzara et al. [11] reported intra-expert variabilities of 20±15% and inter-experts variabilities of 28±12% for manual segmentations of brain tumor images. To alleviate this variability, multiple expert segmentations are combined in an optimal way by using label fusion algorithms such as STAPLE [12], [13]. For classification tasks of brain lesions, the ground truth is obtained with biopsy and pathological tests.

To evaluate performance of a newly developed deep learning approach on a task, it is essential to compare its performance against available state of the art methods. In general, most of the algorithms are evaluated on different sets of data and reported different similarity metrics. This makes it hard to compare the performance of different algorithms against each other. Over the last decade, the brain imaging community has become more aware of this and created publicly available datasets with ground truth for evaluating the performance of algorithms against each other in an unbiased way. One of the first such datasets was released in the framework of an MS lesion segmentation challenge, which was held in conjunction with MICCAI 2008. The dataset is maintained as an online challenge dataset (<https://www.nitrc.org/projects/msseg>), meaning the training data is released with the ground truth to the public, while the test dataset is released without the ground truth and thus can be evaluated only by the organizers. The latter helps avoid overfitting of the methods and makes comparison more objective. Following the same paradigm, many other datasets have been released since then. Some of the other well-known publicly available datasets for brain MRI are Brain Tumor Segmentation (BRATS), Ischemic Stroke Lesion Segmentation (ISLES), Mild Traumatic Brain Injury Outcome Prediction (mTOP), Multiple Sclerosis Segmentation (MSSEG), Neonatal Brain Segmentation (NeoBrainS12), and MR Brain Image Segmentation (MRBrainS).

BRATS: This brain tumor image segmentation challenge in conjunction with the MICCAI conference has been held annually since 2012 in order to evaluate the current state-of-the-art in automated brain tumor segmentation and compare between different methods. For this purpose, a large dataset of brain tumor MR scans and ground truth (5 labels: healthy brain tissue, necrosis, edema, non-enhanced, and enhanced regions of tumors) are made publicly available. The training data has increased over the years. Currently (Brats 2015-2016), the training set comprises 220 subjects with high grade and 54 subjects with low-grade and the test set comprises 53 subjects with mixed grades. All datasets have

been aligned to the same anatomical template and interpolated to 1 mm³ voxel resolution. Each dataset has pre-contrast T1, post contrast T1, T2, and T2 FLAIR MRI volumes. The co-registered, skull-stripped, and annotated training dataset and evaluation results of algorithms are available via the Virtual Skeleton Database (<https://www.virtualskeleton.ch/>).

ISLES: This challenge is organized to evaluate stroke lesion/clinical outcome prediction from acute MRI scans. Acute MRI scans of a large number of acute stroke cases and associated clinical parameters are provided. The associated ground truth is the final lesion volume (Task I) as manually segmented in 3 to 9 month follow-up scans, and the clinical mRM score (Task II) denoting the degree of disability. For ISLES 2016, 35 training and 40 testing cases made publicly available via SMIR platform (<https://www.smir.ch/ISLES/Start2016>). The performance of the winner algorithm on this dataset for subacute ischemic stroke lesion segmentation currently is 0.59±0.31 (Dice similarity coefficient, DSC) and 37.88±30.06 (Hausdorff Distance, HD).

mTOP: This challenge calls for methods that focus on finding differences between healthy subjects and Traumatic Brain Injury (TBI) patients and sort the given data in distinct categories in an unsupervised manner. Publicly available MRI data can be downloaded from <https://tbichallenge.wordpress.com/data>.

MSSEG: The goals of this challenge are evaluating state-of-the-art and advanced segmentation methods from the participants on MS data. For this, they evaluate both lesion detection (how many lesions are detected) and lesion segmentation (how precisely the lesions are delineated) on a multicenter database (38 patients from four different centers, imaged on 1.5 or 3T scanners, each patient being manually annotated by seven experts). In addition to this classical evaluation, they provide a common infrastructure to evaluate the algorithms such as running time comparison and the degree of automation. The data can be obtained from <https://portal.fli-iam.irisa.fr/msseg-challenge/data>.

NeoBrainS12: The aim of the NeoBrainS12 challenge is to compare algorithms for segmentation of neonatal brain tissues and measurement of corresponding volumes using T1 and T2 MRI scans of the brain. The comparison is performed for the following structures: cortical and central grey matter, non-myelinated and myelinated white matter, brainstem and cerebellum, and cerebrospinal fluid in the ventricles and in the extracerebral space. Training set includes T1 and T2 MR images of two infants at 30 and 40 weeks ages. Test set includes T1 and T2 MRI of five infants. The data and evaluation results of algorithms that has been submitted to the challenge can be downloaded from <http://neobrains12.isi.uu.nl/>.

MRBrainS: The aim of the MRBrainS evaluation framework is to compare algorithms for segmentation of grey matter, white matter and cerebrospinal fluid on multi-sequence (T1-weighted, T1-weighted inversion recovery and FLAIR) 3 Tesla MRI scans of the brain. Five brain MRI scans with manual segmentations are provided for training and fifteen only MRI scans are provided for testing. The data can be downloaded from <http://mrbrains13.isi.uu.nl>. The performance (DSC) of the current winner algorithm on this dataset is 86.15% for gray matter, 89.46% for white matter, and 84.25% for cerebrospinal fluid segmentation.

The most common quantitative measures used for evaluation brain MRI segmentation methods are listed below and shown in Table 1. Typically, the methods for normal structure or tumor segmentation include voxel-wise metrics, such as DSC, true positive rate (TPR), positive predictive value (PPV) and lesion surface metrics, such as HD and average symmetric surface distance (ASSD). On the other hand, methods for multifocal brain lesions often also include lesion-wise metrics, such as lesion-wise true positive rate (LTPR) and lesion-wise positive predictive value (LPPV). Measures such as accuracy and

specificity tend to be avoided in the lesion segmentation context since these measures do not discriminate between different segmentation outputs when the object (lesion) is considerably smaller than the background (normal-appearing brain tissue). In addition, measures of clinical relevance are also commonly incorporated. These include such measures as correlation analysis of total lesion load or count as detected by automated and manual segmentation, and volume or volume change correlation. Significance tests commonly accompany contributions that build on or compare to other methods, most often nonparametric tests such as Wilcoxon's signed rank or Wilcoxon's rank sum tests are preferred.

Table 1: A summary of popular quantitative measures of brain MRI segmentation quality and their mathematical formulation with respect to the number of false positives (FP), true positives (TP), false negatives (FN) at voxel level and lesion level (FPL, TPL, and FNL, respectively). ∂S and ∂R are the sets of lesion border pixels/voxels for the tested and the reference segmentations, and $d_m(v, V)$ is the minimum of the Euclidean distances between a voxel v and voxels in a set V .

Metric of segmentation quality	Mathematical description
True positive rate, TPR	$TPR = \frac{TP}{TP + FN}$
Positive predictive rate, PPV	$PPV = \frac{TP}{TP + FP}$
Dice similarity coefficient, DSC	$DSC = \frac{2TP}{2TP + FP + FN}$
Volume difference rate, VDR	$VDR = \frac{ FP - FN }{TP + FN}$
Hausdorff distance	$HD = \max\{\sup_{r \in \partial R} d_m(s, r), \sup_{s \in \partial S} d_m(r, s)\}$
Average symmetric surface distance, ASSD	$ASSD = \frac{\sum_{s \in \partial S} d_m(s, \partial R) + \sum_{r \in \partial R} d_m(r, \partial S)}{ \partial S + \partial R }$
Lesion-wise true positive rate, LTPR	$LTPR = \frac{TPL}{TPL + FNL}$
Lesion-wise positive predictive value, LPPV	$LPPV = \frac{TPL}{TPL + FPL}$

2.2. Image Preprocessing

Automated analysis of MR images is challenging due to intensity inhomogeneity, variability of the intensity ranges and contrast, and noise. Therefore, prior to automated analysis, certain steps are required to make the images appear more similar, and these steps are commonly referred to as preprocessing. Typical preprocessing steps for structural brain MRI include the following key steps.

Registration: Spatial alignment of the images to a common anatomical space [14]. Interpatient image registration aids in standardizing the MR images onto a standard stereotaxic space, commonly MNI or ICBM. Intrapatient registration aims to align the images of different sequences, e.g. T1 and T2, to obtain a multi-channel representation for each location within the brain.

Skull stripping: Removing the skull from images to focus on intracranial volume. The most common methods used for this purpose have been BET [15], Robex [16], and SPM [16], [17].

1
2
3
4 **Bias field correction:** Correction of the image contrast variations due to magnetic field
5 inhomogeneity [18]. The most commonly adopted approach is N4 bias field correction.
6

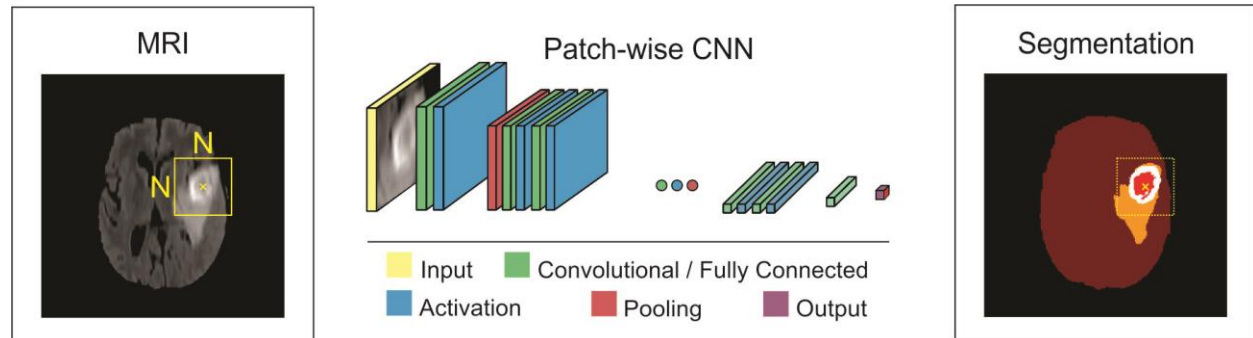
7 **Intensity normalization:** Mapping intensities of all images into a standard or reference scale,
8 e.g., between 0-4095. The algorithm by Nyul et al. [19], which uses piecewise linear mapping of image
9 intensities into a reference scale, is one of the most popular normalization techniques. In the context of
10 deep learning frameworks, computing z-scores, where one subtracts the mean image intensity from all
11 pixels in an image and divides pixels by the standard deviation of intensities, is another popular
12 normalization technique.
13

14 **Noise reduction:** Reduction of the locally-variant Rician noise observed in MR images [20].
15

16 With advent of deep learning techniques, some of the preprocessing steps became less critical
17 for the final segmentation performance. For instance, bias correction and quantile-based intensity
18 normalization are often successfully replaced by the z-score computation alone [2], [21], however,
19 another work shows improvement when applying normalization prior to deep learning based
20 segmentation procedure [22]. At the same time, the new methods for these preprocessing routines are
21 also arising, including deep learning based registration [23], skull stripping [24], and noise reduction [25].
22
23

24 2.3. Current CNN Architecture Styles 25

26 **Patch-wise CNN architecture:** This is a simple approach to train a CNN algorithm for segmentation.
27 An NxN patch around each pixel is extracted from a given image, and the model is trained on these
28 patches and given class labels to correctly identify classes such as normal brain and tumor. The designed
29 networks contain multiple convolutional, activation, pooling and fully connected layers sequentially. Most
30 of the current popular architectures [21], [22], [26], [27] use this approach. To improve the performance
31 of patch-wise architectures, multiscale CNNs [28], [29] use multiple pathways, where each uses a patch
32 of different size around the same pixel. The output of these pathways are combined by a neural network
33 and the model trained to correctly identify the given class labels.
34
35



47 **Figure 2.** Schematic illustration of a patch-wise CNN architecture for brain tumor segmentation task.
48

49 **Semantic-wise CNN architecture:** This type of architecture makes predictions for each pixel of the
50 whole input image like semantic segmentation [37], [55]. Similar to autoencoders, they include encoder
51 part that extracts features and decoder part that upsamples or deconvolves the higher level features from
52 the encoder part and combines lower level features from the encoder part to classify pixels. The input
53 image is mapped to the segmentation labels in a way that minimizes a loss function.
54
55
56
57
58
59
60
61
62
63
64
65

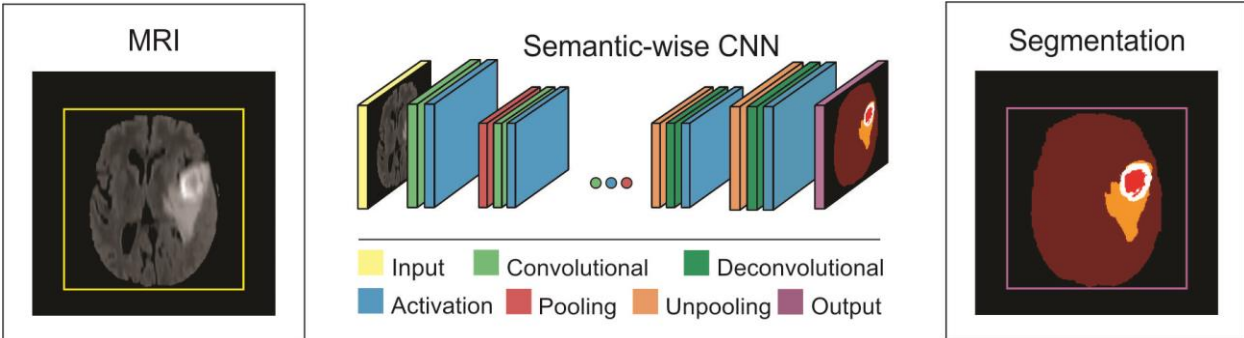


Figure 3. Schematic illustration of a semantic-wise CNN architecture for brain tumor segmentation task.

Cascaded CNN architecture: This type of architecture combines two CNN architectures [56]. The output of the first CNN is used as an input to the second CNN to obtain classification results. The first CNN is used to train the model with initial prediction of class labels while second CNN is used to further tune the results of the first CNN.

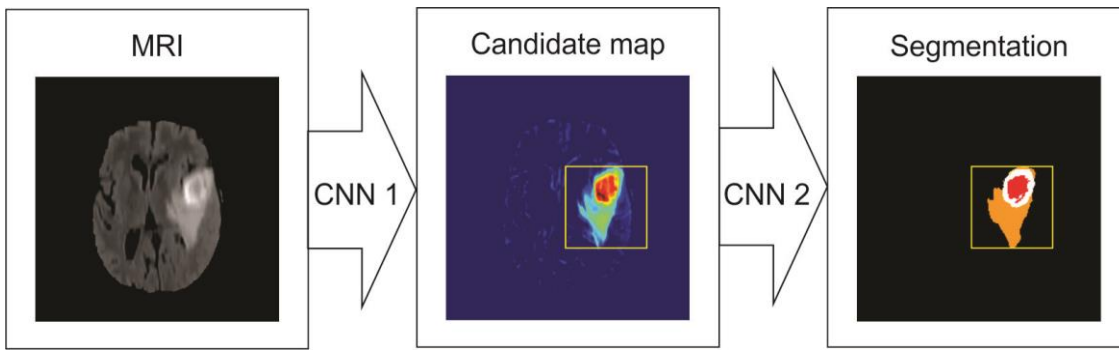


Figure 4. Schematic illustration of a cascaded CNN architecture for brain tumor segmentation task, where the output of the first network (CNN 1) is used in addition to image data for a refined input to the second network (CNN 2), which provides final segmentation.

2.4. Segmentation of Normal Brain Structure

Accurate automated segmentation of brain structures, e.g. white matter (WM), gray matter (GM), and cerebrospinal fluid (CSF), in MRI is important for studying early brain developments in infants and quantitative assessment of the brain tissue and intracranial volume in large scale studies. Atlas based approaches [30]–[33], which match intensity information between an atlas and target images, and pattern recognition approaches [34]–[36], which classify tissues based on a set of local intensity features, are the classical approaches that have been used for brain tissue segmentation. In recent years, CNNs have been adopted for segmentation of brain tissues, which avoid the explicit definition of spatial and intensity features and provide better performance than classical approaches, as we describe next (see Table 2 for the list of studies).

Zhang et al. [27] presented a 2D (input patch size 13-by-13 pixels) patch-wise CNN approach to segment WM, GM, and CSF from multimodal (i.e. T1, T2, and fractional anisotropy) MR images of infants. They showed that their CNN approach outperforms prior methods and classical machine learning algorithms using support vector machine (SVM) and random forest (RF) classifiers (overall DSC performance: $85.03\% \pm 2.27\%$ (CNN) vs. $76.95\% \pm 3.55\%$ (SVM), $83.15\% \pm 2.52\%$ (RF)). Nie et al. [37] presented a semantic-wise fully convolutional networks (FCNs) to segment infant brain images from the

same dataset that Zhang et al. [27] used in their study. They obtained improved results compared to [27]. Their overall DSC were 85.5% (CSF), 87.3% (GM), and 88.7% (WM) vs. 83.5% (CSF), 85.2 (GM) and 86.4 (WM) by [27]. De Brebisson et al. [38] presented a 2D ($I = 29^2$) and 3D ($I = 13^3$) patch-wise CNN approach to segment human brain to anatomical regions. They achieved competitive results (DSC = $72.5\% \pm 16.3\%$) in MICCAI 2012 challenge on multi-atlas labeling as the first CNN approach applied to the task. Moeskops et al. [28] presented a multi-scale ($25^2, 51^2, 75^2$ pixels) patch-wise CNN approach to segment brain images of infants and young adults. They obtained overall DSC = 73.53% vs. 72.5% by [38] in MICCAI challenge on multi-atlas labelling. Bao et al. [39] also presented a multi-scale patch-wise CNN together with dynamic random walker with decay region of interest to obtain smooth segmentation of subcortical structures in IBSR (developed by the Centre for Morphometric Analysis at Massachusetts General Hospital-available at <https://www.nitrc.org/projects/ibsr> to download) and LPBA40 [40] datasets. They reported overall DSC of 82.2% and 85% for IBSR and LPBA40, respectively. CNN-based deep learning approaches have shown the top performances on NeoBrainS12 and MRBrainS (see Table 3) challenges. Their computation time at testing phase was also much less than classical machine learning algorithms.

Table 2: Deep learning approaches for brain structure segmentation

Authors	CNN Style	Dim	Accuracy	Data
Zhang et al. 2015	patch-wise	2D	DSC: 83.5% (CSF), 85.2% (GM), 86.4% (WM)	Private data (10 healthy infants)
Nie et al. 2016	semantic-wise	2D	DSC: 85.5% (CSF), 87.3% (GM), 88.7% (WM)	Private data (10 healthy infants)
de Brebisson et al. 2015	patch-wise	2D/3D	overall DSC: $72.5\% \pm 16.3\%$	MICCAI 2012-multi-atlas labelling
Moeskops et al. 2016	patch-wise	2D/3D	overall DSC: 73.53%	MICCAI 2012-multi-atlas labelling
Bao et al. 2016	patch-wise	2D	DSC: 82.2% / 85%	IBSR/LPBA40

Table 3: Top 10 ranking of algorithms in MRBrainS challenge (Complete list is available at: <http://mrbrains13.isi.uu.nl/results.php>)

Rank	Team name	Submission name	Sequence used	Speed
1	CU_DL	3D Deep Learning; voxnet1	T1;T1_IR;FLAIR	~2 min
2	CU_DL2	3D Deep Learning; voxnet2	T1;T1_IR;FLAIR	~2 min
3	MDGRU	Multi-Dimensional Gated Recurrent Units	T1;T1_IR;FLAIR	~2 min
4	PyraMiD-LSTM2	NOCC with rounds	T1;T1-IR;FLAIR	~2 min
5	FBI/LMB Freiburg	U-Net (3D)	T1;T1-IR;F	~2 min
6	IDSIA	PyraMiD-LSTM	T1;T1_IR;FLAIR	~2 min
7	STH	Hybrid ANN-based Auto-context method	T1;T1-IR;FLAIR	~ 5 min
8	ISI-Neonatology	Multi-stage voxel classification	T1	~1.5hours

9	UNC-IDEA	LINKS:Learning-based multi-source integration	T1;T1_IR;FLAIR	~3 min
10	MNAB2	Random Forests	T1;T1_IR;FLAIR	~25 min

2.5. Segmentation of Brain Lesions

Quantitative analysis of brain lesions include measurement of established imaging biomarkers such as the largest diameter, volume, count, and progression, to quantify treatment response of the associated diseases, such as brain cancer, MS, stroke, etc. Reliable extraction of these biomarkers depends on prior accurate segmentation. Despite the significant effort in brain lesion segmentation and advanced imaging techniques, accurate segmentation of brain lesions remains a challenge. Many automated methods have been proposed for lesion segmentation problem, including unsupervised modeling methods that aim to automatically adapt to new image data [41]–[43] supervised machine learning methods that, given a representative dataset, learn the textural and appearance properties of lesions [44], and atlas-based methods that combine both supervised and unsupervised learning into a unified pipeline by registering labeled data or a known cohort data into a common anatomical space [45]–[47]. Several review papers provide overview of classical methods for brain tumor segmentation [48], and MS lesion segmentation [49], [50]. For more information and detail on the classical approaches we refer the reader to those studies.

Several deep learning studies have shown superior performances to the classical state-of-art methods (see Table 4). Havaei et al. [26] presented a 2D (33x33 pixels) patch-wise architecture using local and global CNN pathways, which exploits local and global contextual features around a pixel to segment brain tumors. The local pathway includes two convolutional layers with kernel sizes of 7x7 and 5x5 respectively while the global pathway includes one convolutional layer with kernel size of 11x11. To tackle the difficulties raised by imbalance of tumor vs. normal brain labels, where the fraction of latter is above 90% of total samples, they introduced two phase training which included training first with data that had equal class probability and then training only the output layer with the unbalanced data (i.e. keeping the weights of all the other layers unchanged). They also explored cascaded architectures in their study. They reported that their CNN approach outperformed and was much faster at testing phase (3min vs. 100 mins) than the winner of BRATS 2013 competition.

In another study, Havaei et al. [51] presented an overview of brain tumor segmentation with deep learning, which also described the use of cascaded architecture. Pereira et al. [22] presented a 2D patch-wise architecture, but compared to Havaei et al., they used small 3x3 convolutional kernels which allowed deeper architectures, patch intensity normalization, and data augmentation by rotation of patches. They also designed two separate models for each grade – high-grade (HG) and low-grade (LG) tumors. The model for HG tumors included six convolutional layers and three fully connected layers while the model for LG included four convolutional layers and three fully connected layers. They also used leaky ReLU for activation function, which allowed gradient flow in contrast to rectified linear units that impose constant zero to negative values. Their method showed the best performance on the Brats 2013 data – DSC values of 0.88, 0.83, 0.77 for complete, core, and enhancing regions, respectively. They were also ranked as second place in Brats 2015 data. Zhao and Jia [52] also used a patch-wise CNN architecture using triplanar (axial, sagittal, coronal) 2D slices to segment brain tumors. They have obtained comparable results to state-of-art machine learning algorithms on Brats 2013 data. Kamnitsas et al. [21] presented a 3D dense-inference patch-wise and multi-scale CNN architecture that uses 3D (3x3x3 pixels) convolutional kernels and two pathway learning similar to [26]. They also used a 3D fully connected conditional random field to effectively remove false positives, which is an important post-processing step that was not described in previous studies. They reported the top ranking performance on Brats 2015. Dvorak et al. [53] presented a 2D patch-wise CNN approach that mapped input patches to n groups of structured local predictions that took into account the labels of the neighboring pixels. They reported

results on Brats 2014 data that were comparable to those of state-of-art approaches. Most of these studies have also been presented in last two MICCAI conference as part of the BRATS challenge. We refer the reader to BRATS proceedings 2015-2016 [54] for further details such as performance comparison and ranking

CNN-based deep learning architectures have also been used for segmentation of stroke and MS lesions, detection of cerebral microbleeds, and prediction of therapy response. Brosch et al. [55] presented a 3D semantic-wise CNN to segment MS lesions from MRI. They evaluated their method on two publicly available datasets, MICCAI 2008 and ISBI 2015 challenges, and compared their method to freely available and widely used segmentation methods. They reported performance comparable to the state of the art methods and superior to the publicly available MS segmentation methods. Dou et al. [56] presented a cascaded framework that included 3D semantic-wise CNN and a 3D patch-wise CNN to detect cerebral microbleeds (CM) from MRI. They reported their method outperformed previous studies with low level descriptors and provided a high sensitivity of 93.2% for detecting CM. Maier et al. [57] presented a comparison study that evaluated and compared nine classification methods (e.g. naive Bayes, random forest, and CNN) for ischemic stroke lesion segmentation. Their results showed that cascaded CNN and random decision forest approaches outperforms all other methods. Akkus et al. [29] presented prediction of 1p19q chromosomal co-deletion, which is associated with positive response to treatment in low grade gliomas from MRI using a 2D patch-wise and multi-scale CNN. The performance of their CNN approach on an unseen test set was 93.3% (sensitivity) and 82.22% (specificity) for detection of 1p19q status from MRI.

Table 4: Deep learning approaches for quantification of brain lesions

Authors	Aim	CNN Style	Dim	Accuracy	Dataset
Havaei et al. 2016	Tumor segmentation	patch-wise	2D	DSC: 0.88 (Complete), 0.79 (Core), 0.73 (Enhancing)	BRATS-2013
S. Pereira et al. 2016	Tumor segmentation	patch-wise	2D	DSC: 0.88 (Complete), 0.83 (Core), 0.77 (Enhancing)	BRATS-2013
(Zhao and Jia 2015	Tumor segmentation	patch-wise	2D	Overall accuracy: 0.81	BRATS-2013
Kamnitsas et al. 2016	Tumor segmentation	patch-wise	3D	DSC: 0.9 (Complete), 0.75 (Core), 0.73 (Enhancing)	BRATS-2015
Dvorak et al. 2015	Tumor segmentation	patch-wise	2D	DSC: 0.83 (Complete), 0.75 (Core), 0.77 (Enhancing)	BRATS-2014
Brosch et al. 2016	MS segmentation	semantic-wise	3D	DSC:0.68 (ISBI); DSC:0.84 (MICCAI)	MICCAI 2008- ISBI 2015
Dou et al. 2016	Cerebral microbleed detection	cascaded (semantic/patch-wise)	3D	Sensitivity: 98.29%	private data (320 subjects)
Maier et al. 2015	Ischemic stroke detection	patch-wise	2D	DSC: 0.67 ± 0.18 ; HD: 29.64 ± 24.6	private data (37 subjects)
Akkus et al. 2016	Tumor genomic prediction	patch-wise	2D	0.93 (sensitivity), 0.82 (specificity), and 0.88 (accuracy)	private data (159 subjects)

3. Discussion

The recent advances reported in literature indicate significant potential for deep learning techniques in the field of quantitative brain MR image analysis. Even though deep learning approaches have been applied to brain MRI only recently, they tend to outperform previous state of the art classical machine learning algorithms and are becoming more mature. Brain image analysis has been a great challenge to computer-aided techniques due to complex brain anatomy and variability of its appearance, non-standardized MR scales due to variability in imaging protocols, image acquisition imperfection, and presence of pathology. Therefore, there is a need for more generic techniques such as deep learning that would handle these variabilities.

Despite a significant breakthrough, the potential of deep learning is limited because the medical imaging datasets are relatively small and this limits the ability of the methods to manifest their full power, compared to what they have demonstrated on large-scale datasets (e.g. millions of images) such as ImageNet. While some authors report that their supervised frameworks require only one training sample [28], most researchers report that their results were consistently improving with an increase in size of training datasets [58], [59]. There is high demand for large-scale datasets for effective application of deep learning methods. Alternatively, the size of the dataset can be effectively increased by applying random transformations to the original data such as flipping, rotation, translation, and deformation. This is commonly used in machine learning and known as data augmentation. Data augmentation helps increase the size of training examples and reduce overfitting by introducing random variations to the original data. Multiple studies have reported the data augmentation to be very useful in their studies [7], [22], [29].

Several steps are crucial to improve the learning with deep learning approaches, including data preprocessing, data post-processing, network weight initialization, and strategies to prevent overfitting. Image preprocessing plays a key role in learning. Multiple preprocessing steps have been applied in current studies to improve learning process, as presented in Sections 2.5 and 2.6. For example, it is important to have intensities of input brain MR images in a reference scale and normalized for each modality. This avoids suppression of true patterns of structures by any modality and intensity differences in the output of the model. Post-processing of the output of model is also an important step to refine the segmentation results. The goal of any learning method is to have a perfect classification, but there are always regions in images that overlap between classes, known as partial volume effect, which unavoidably leads to false positives or negatives. These regions require additional processing for accurate quantification. Another important step is proper network parameter initialization in the neural network to maintain the gradient flow through network and to achieve convergence. Otherwise, the activations and gradient flow can vanish and result in no convergence and learning. Random weight initialization has been used in most of the current studies. Lastly, preventing overfitting is critical to learn the true information in images, and avoiding overfitting to specific training examples provided. Deep networks are particularly susceptible to overfitting because several thousands or millions of parameters are used in the networks and limited training data is available. Several strategies have been used to prevent overfitting such as data augmentation that introduces random variations to input data [7], [22], [29], using dropout that randomly removes nodes from network during training [22], [53], [56], and L1/L2 regularization that introduces weight penalties [26]. In current deep learning architectures, one or more of these strategies are used to prevent overfitting.

Semantic-wise architectures take inputs of any size and produce a classification map while patch-wise CNN architectures take fixed-sized inputs and produce non-spatial outputs. Therefore, semantic-wise architectures produce results for each pixel/voxel of an image much faster than patch-wise architectures. As presented in [60], it takes 22ms to produce 10x10 grid of output from 500x500 input image for semantic-wise FCN while it takes 1.2ms for patch-wise AlexNet [7] to infer a single value

classification output of a 227x227 image, which is more than 5 times improvement in computation speed (22ms vs. 120ms). On the other hand, random sampling of patches over a dataset potentially results in faster convergence (LeCun et al. 1998) compared to full image training in semantic-wise architectures. Semantic-wise architectures also are more susceptible to class imbalance but this can be solved by weighting the classes in the loss function [55]. Cascaded architectures such as a patch-wise architecture following a semantic architecture as used in [56] would resolve the issues raised by each approach and refine the output results.

Developing a generic deep learning approach that will work on datasets from different machines and institutions is challenging due to limited training and ground truth data, variations and image acquisition protocols, imperfections of each MRI scanner, and variations in appearance of healthy and pathological brain tissue. So far, currently available methods were randomly initialized and trained on a limited data. To improve the generalization of deep learning architectures, one can adapt a well performing deep learning network trained on a large dataset and fine-tune that network on a smaller dataset specific to the problem, which is called transfer learning. It has been shown that transferring the weights (network parameters) from a pre-trained generic network to train on a specific dataset is better than random weight initialization of the network [61]. The usefulness and success of transfer learning depends on similarity between datasets. For instance, using pre-trained models from ImageNet, which is trained on a large RGB image database, might not perform well on medical images without further training. Shin et al. [62] reported that they obtained best performance with transfer learning from pre-trained model on ImageNet dataset and fine-tuning on lymph node and interstitial lung disease rather than training from scratch. On the other hand, the nature of the ImageNet dataset is much different than medical image dataset and therefore transfer learning from ImageNet might not be the best choice for medical images as shown in [63].

4. Summary

Despite the significant impact of deep learning techniques in quantitative brain MRI, it is still challenging to have a generic method that will be robust to all variations in brain MR images from different institutions and MRI scanners. The performance of the deep learning methods depends highly on several key steps such as preprocessing, initialization, and post-processing. Also, training datasets are relatively small compared to large-scale ImageNet dataset (e.g. millions of images) to achieve generalization across datasets. Moreover, current deep learning architectures are based on supervised learning and require generation of manual ground truth labels, which is tedious work on a large-scale data. Therefore, deep learning models that are highly robust to variations in brain MRI or have unsupervised learning capability with less requirement on ground truth labels are needed. In addition, data augmentation approaches that realistically mimic variations in brain MRI data could alleviate the need of large amount of data. Transfer learning could be used to share well-performing deep learning models, which are trained on normal and pathological brain MRI data, among brain imaging research community and improve the generalization ability of these models across datasets with less effort than learning from scratch.

Acknowledgements:

This work was supported by National Institutes of Health 1U01CA160045, U01CA142555, 1U01CA190214, and 1U01CA187947.

Conflict Of Interest:

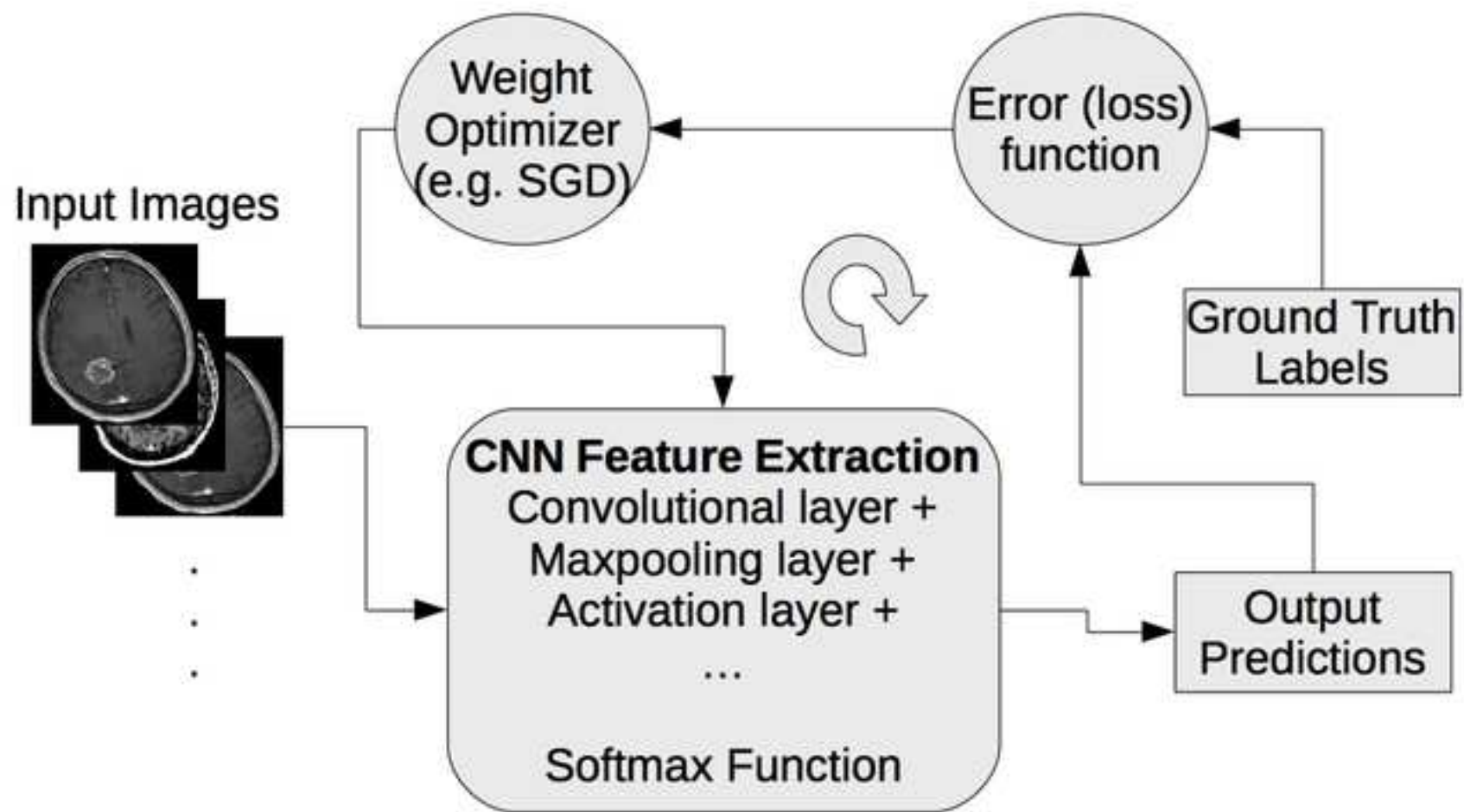
The authors declare that there is no conflict of interest.

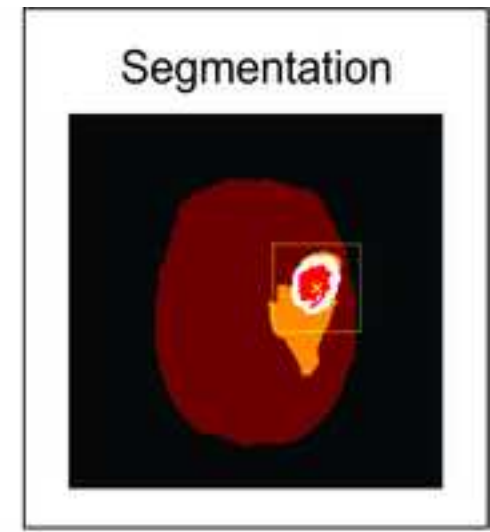
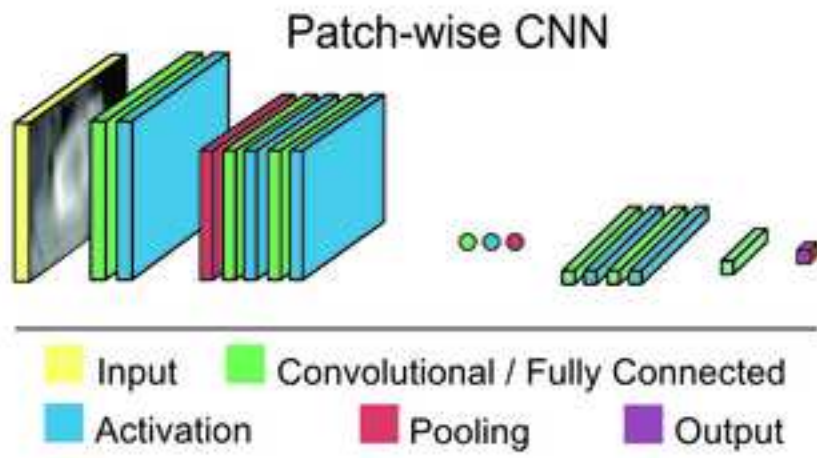
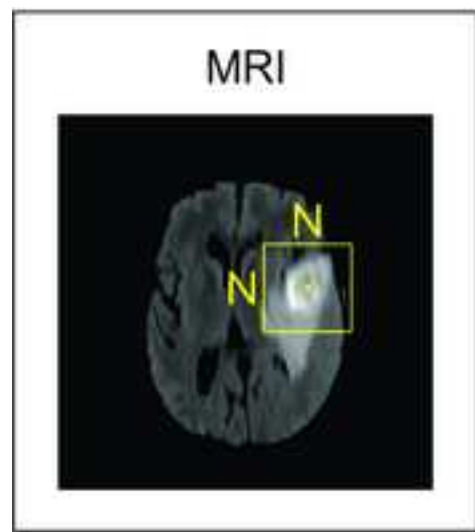
References:

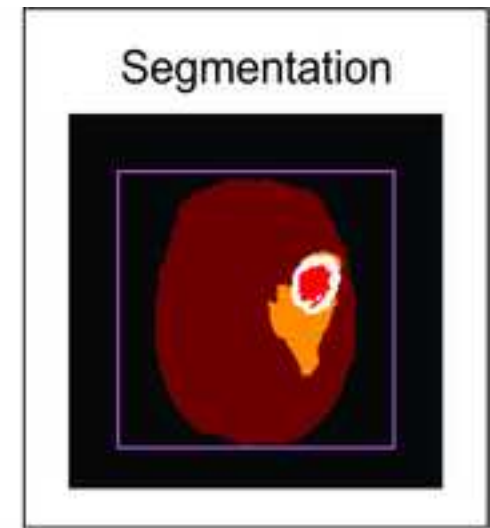
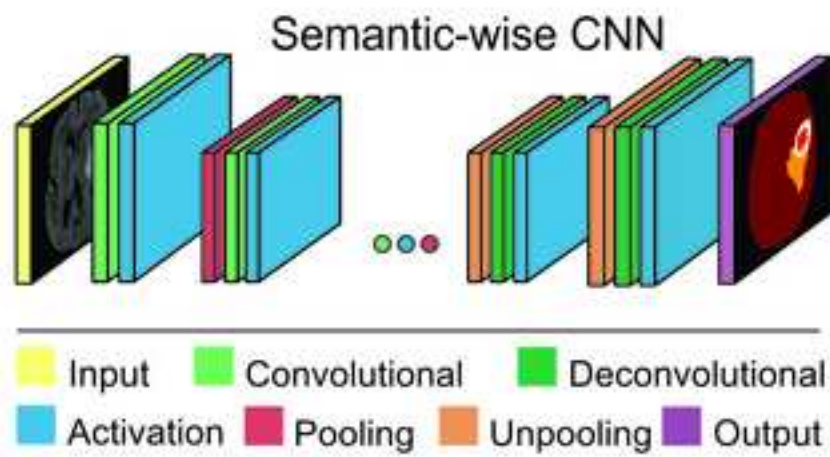
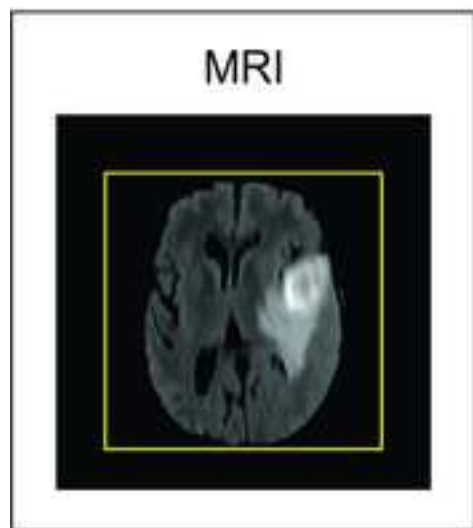
- [1] Y. LeCun, Y. Bengio, and G. Hinton, "Deep learning," *Nature*, vol. 521, no. 7553, pp. 436–444, May 2015.
- [2] D. Lin, A. V. Vasilakos, Y. Tang, and Y. Yao, "Neural networks for computer-aided diagnosis in medicine: A review," *Neurocomputing*, vol. 216, pp. 700–708, Dec. 2016.
- [3] T. Kooi et al., "Large scale deep learning for computer aided detection of mammographic lesions," *Med. Image Anal.*, vol. 35, pp. 303–312, Jan. 2017.
- [4] J.-Z. Cheng et al., "Computer-Aided Diagnosis with Deep Learning Architecture: Applications to Breast Lesions in US Images and Pulmonary Nodules in CT Scans," *Sci. Rep.*, vol. 6, p. 24454, Apr. 2016.
- [5] G. Litjens et al., "Deep learning as a tool for increased accuracy and efficiency of histopathological diagnosis," *Sci. Rep.*, vol. 6, p. 26286, May 2016.
- [6] Y. LeCun et al., "Backpropagation Applied to Handwritten Zip Code Recognition," *Neural Comput.*, vol. 1, no. 4, pp. 541–551, 1989.
- [7] A. Krizhevsky, I. Sutskever, and G. E. Hinton, "ImageNet Classification with Deep Convolutional Neural Networks," in *Advances in Neural Information Processing Systems 25*, F. Pereira, C. J. C. Burges, L. Bottou, and K. Q. Weinberger, Eds. Curran Associates, Inc., 2012, pp. 1097–1105.
- [8] Jia Deng et al., "ImageNet: A large-scale hierarchical image database," in *2009 IEEE Conference on Computer Vision and Pattern Recognition*, 2009.
- [9] O. Russakovsky et al., "ImageNet Large Scale Visual Recognition Challenge," *Int. J. Comput. Vis.*, vol. 115, no. 3, pp. 211–252, 2015.
- [10] K. He, X. Zhang, S. Ren, and J. Sun, "Delving Deep into Rectifiers: Surpassing Human-Level Performance on ImageNet Classification," in *2015 IEEE International Conference on Computer Vision (ICCV)*, 2015.
- [11] G. P. Mazzara, R. P. Velthuizen, J. L. Pearlman, H. M. Greenberg, and H. Wagner, "Brain tumor target volume determination for radiation treatment planning through automated MRI segmentation," *Int. J. Radiat. Oncol. Biol. Phys.*, vol. 59, no. 1, pp. 300–312, May 2004.
- [12] S. K. Warfield, K. H. Zou, and W. M. Wells, "Simultaneous Truth and Performance Level Estimation (STAPLE): An Algorithm for the Validation of Image Segmentation," *IEEE Trans. Med. Imaging*, vol. 23, no. 7, pp. 903–921, 2004.
- [13] A. Akhondi-Asl, L. Hoyte, M. E. Lockhart, and S. K. Warfield, "A logarithmic opinion pool based STAPLE algorithm for the fusion of segmentations with associated reliability weights," *IEEE Trans. Med. Imaging*, vol. 33, no. 10, pp. 1997–2009, Oct. 2014.
- [14] A. Klein et al., "Evaluation of 14 nonlinear deformation algorithms applied to human brain MRI registration," *Neuroimage*, vol. 46, no. 3, pp. 786–802, Jul. 2009.
- [15] S. M. Smith, "Fast robust automated brain extraction," *Hum. Brain Mapp.*, vol. 17, no. 3, pp. 143–155, Nov. 2002.
- [16] J. E. Iglesias, C.-Y. Liu, P. M. Thompson, and Z. Tu, "Robust brain extraction across datasets and comparison with publicly available methods," *IEEE Trans. Med. Imaging*, vol. 30, no. 9, pp. 1617–1634, Sep. 2011.
- [17] J. Ashburner and K. J. Friston, "Unified segmentation," *Neuroimage*, vol. 26, no. 3, pp. 839–851, Jul. 2005.
- [18] U. Vovk, F. Pernus, and B. Likar, "A review of methods for correction of intensity inhomogeneity in MRI," *IEEE Trans. Med. Imaging*, vol. 26, no. 3, pp. 405–421, Mar. 2007.
- [19] L. G. Nyúl and J. K. Udupa, "On standardizing the MR image intensity scale," *Magn. Reson. Med.*, vol. 42, no. 6, pp. 1072–1081, 1999.
- [20] P. Coupe, P. Yger, S. Prima, P. Hellier, C. Kervrann, and C. Barillot, "An optimized blockwise nonlocal means denoising filter for 3-D magnetic resonance images," *IEEE Trans. Med. Imaging*, vol. 27, no. 4, pp. 425–441, Apr. 2008.
- [21] K. Kamnitsas et al., "Efficient multi-scale 3D CNN with fully connected CRF for accurate brain lesion segmentation," *Med. Image Anal.*, vol. 36, pp. 61–78, Oct. 2016.
- [22] S. Pereira, A. Pinto, V. Alves, and C. A. Silva, "Brain Tumor Segmentation using Convolutional Neural Networks in MRI Images," *IEEE Trans. Med. Imaging*, Mar. 2016.
- [23] G. Wu, M. Kim, Q. Wang, Y. Gao, S. Liao, and D. Shen, "Unsupervised deep feature learning for deformable registration of MR brain images," *Med. Image Comput. Comput. Assist. Interv.*, vol. 16, no. Pt 2, pp. 649–656, 2013.
- [24] J. Kleesiek et al., "Deep MRI brain extraction: A 3D convolutional neural network for skull stripping,"

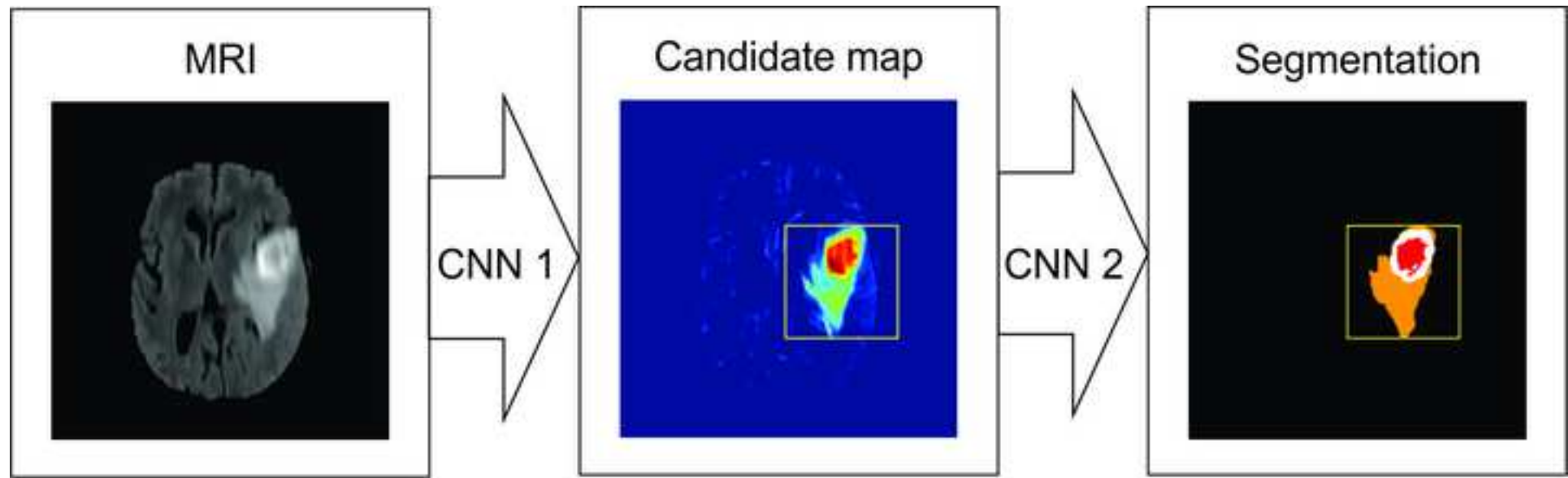
- 1 Neuroimage, vol. 129, pp. 460–469, Apr. 2016.
- 2 [25] L. Gondara, “Medical image denoising using convolutional denoising autoencoders,” arXiv [cs.CV],
- 3 16-Aug-2016.
- 4 [26] M. Havaei et al., “Brain tumor segmentation with Deep Neural Networks,” Med. Image Anal., vol. 35,
- 5 pp. 18–31, May 2016.
- 6 [27] W. Zhang et al., “Deep convolutional neural networks for multi-modality isointense infant brain image
- 7 segmentation,” Neuroimage, vol. 108, pp. 214–224, Mar. 2015.
- 8 [28] P. Moeskops et al., “Automatic Segmentation of MR Brain Images With a Convolutional Neural
- 9 Network,” IEEE Trans. Med. Imaging, vol. 35, no. 5, pp. 1252–1261, 2016.
- 10 [29] Z. Akkus et al., “Predicting 1p19q Chromosomal Deletion of Low-Grade Gliomas from MR Images
- 11 using Deep Learning,” arXiv [cs.CV], 21-Nov-2016.
- 12 [30] V. Srhoj-Egekher, Manon J N, M. A. Viergever, and I. Išgum, “Automatic neonatal brain tissue
- 13 segmentation with MRI,” in Medical Imaging 2013: Image Processing, 2013.
- 14 [31] P. Anbeek et al., “Automatic segmentation of eight tissue classes in neonatal brain MRI,” PLoS One,
- 15 vol. 8, no. 12, p. e81895, Dec. 2013.
- 16 [32] H. A. Vrooman et al., “Multi-spectral brain tissue segmentation using automatically trained k-Nearest-
- 17 Neighbor classification,” Neuroimage, vol. 37, no. 1, pp. 71–81, Aug. 2007.
- 18 [33] A. Makropoulos et al., “Automatic whole brain MRI segmentation of the developing neonatal brain,”
- 19 IEEE Trans. Med. Imaging, vol. 33, no. 9, pp. 1818–1831, Sep. 2014.
- 20 [34] L. Wang et al., “LINKS: learning-based multi-source IntegratioN framework for Segmentation of
- 21 infant brain images,” Neuroimage, vol. 108, pp. 160–172, Mar. 2015.
- 22 [35] P. Moeskops et al., “Automatic segmentation of MR brain images of preterm infants using
- 23 supervised classification,” Neuroimage, vol. 118, pp. 628–641, Sep. 2015.
- 24 [36] S. M. Chiță, M. Benders, P. Moeskops, K. J. Kersbergen, M. A. Viergever, and I. Išgum, “Automatic
- 25 segmentation of the preterm neonatal brain with MRI using supervised classification,” in Medical
- 26 Imaging 2013: Image Processing, 2013.
- 27 [37] D. Nie, N. Dong, W. Li, G. Yaozong, and S. Dinggang, “Fully convolutional networks for multi-
- 28 modality isointense infant brain image segmentation,” in 2016 IEEE 13th International Symposium
- 29 on Biomedical Imaging (ISBI), 2016.
- 30 [38] A. de Brebisson and M. Giovanni, “Deep neural networks for anatomical brain segmentation,” in
- 31 2015 IEEE Conference on Computer Vision and Pattern Recognition Workshops (CVPRW), 2015.
- 32 [39] S. Bao, B. Siqi, and A. C. S. Chung, “Multi-scale structured CNN with label consistency for brain MR
- 33 image segmentation,” Computer Methods in Biomechanics and Biomedical Engineering: Imaging &
- 34 Visualization, pp. 1–5, 2016.
- 35 [40] D. W. Shattuck et al., “Construction of a 3D probabilistic atlas of human cortical structures,”
- 36 Neuroimage, vol. 39, no. 3, pp. 1064–1080, Feb. 2008.
- 37 [41] C. H. Sudre, M. J. Cardoso, W. H. Bouvy, G. J. Biessels, J. Barnes, and S. Ourselin, “Bayesian
- 38 model selection for pathological neuroimaging data applied to white matter lesion segmentation,”
- 39 IEEE Trans. Med. Imaging, vol. 34, no. 10, pp. 2079–2102, Oct. 2015.
- 40 [42] A. Galimzianova, F. Pernuš, B. Likar, and Ž. Špiclin, “Stratified mixture modeling for segmentation of
- 41 white-matter lesions in brain MR images,” Neuroimage, vol. 124, no. Pt A, pp. 1031–1043, Jan.
- 42 2016.
- 43 [43] N. Weiss, D. Rueckert, and A. Rao, “Multiple sclerosis lesion segmentation using dictionary learning
- 44 and sparse coding,” Med. Image Comput. Comput. Assist. Interv., vol. 16, no. Pt 1, pp. 735–742,
- 45 2013.
- 46 [44] Z. Karimaghloo, H. Rivaz, D. L. Arnold, D. L. Collins, and T. Arbel, “Temporal Hierarchical Adaptive
- 47 Texture CRF for Automatic Detection of Gadolinium-Enhancing Multiple Sclerosis Lesions in Brain
- 48 MRI,” IEEE Trans. Med. Imaging, vol. 34, no. 6, pp. 1227–1241, Jun. 2015.
- 49 [45] X. Tomas-Fernandez and S. K. Warfield, “A Model of Population and Subject (MOPS) Intensities
- 50 With Application to Multiple Sclerosis Lesion Segmentation,” IEEE Trans. Med. Imaging, vol. 34, no.
- 51 6, pp. 1349–1361, Jun. 2015.
- 52 [46] N. Shiee, P.-L. Bazin, A. Ozturk, D. S. Reich, P. A. Calabresi, and D. L. Pham, “A topology-
- 53 preserving approach to the segmentation of brain images with multiple sclerosis lesions,”
- 54 Neuroimage, vol. 49, no. 2, pp. 1524–1535, Jan. 2010.
- 55 [47] M. Prastawa, E. Bullitt, S. Ho, and G. Gerig, “A brain tumor segmentation framework based on
- 56 outlier detection,” Med. Image Anal., vol. 8, no. 3, pp. 275–283, Sep. 2004.

- [48] S. Bauer, R. Wiest, L.-P. Nolte, and M. Reyes, "A survey of MRI-based medical image analysis for brain tumor studies," *Phys. Med. Biol.*, vol. 58, no. 13, pp. R97–129, Jul. 2013.
- [49] X. Lladó et al., "Automated detection of multiple sclerosis lesions in serial brain MRI," *Neuroradiology*, vol. 54, no. 8, pp. 787–807, Aug. 2012.
- [50] D. García-Lorenzo, S. Francis, S. Narayanan, D. L. Arnold, and D. L. Collins, "Review of automatic segmentation methods of multiple sclerosis white matter lesions on conventional magnetic resonance imaging," *Med. Image Anal.*, vol. 17, no. 1, pp. 1–18, Jan. 2013.
- [51] M. Havaei, N. Guizard, H. Larochelle, and P.-M. Jodoin, "Deep Learning Trends for Focal Brain Pathology Segmentation in MRI," in *Lecture Notes in Computer Science*, 2016, pp. 125–148.
- [52] L. Zhao and K. Jia, "Deep Feature Learning with Discrimination Mechanism for Brain Tumor Segmentation and Diagnosis," in *2015 International Conference on Intelligent Information Hiding and Multimedia Signal Processing (IHIH-MSP)*, 2015.
- [53] P. Dvořák, D. Pavel, and M. Bjoern, "Local Structure Prediction with Convolutional Neural Networks for Multimodal Brain Tumor Segmentation," in *Lecture Notes in Computer Science*, 2016, pp. 59–71.
- [54] B. H. Menze et al., "The Multimodal Brain Tumor Image Segmentation Benchmark (BRATS)," *IEEE Trans. Med. Imaging*, vol. 34, no. 10, pp. 1993–2024, Oct. 2015.
- [55] T. Brosch et al., "Deep 3D Convolutional Encoder Networks With Shortcuts for Multiscale Feature Integration Applied to Multiple Sclerosis Lesion Segmentation," *IEEE Trans. Med. Imaging*, vol. 35, no. 5, pp. 1229–1239, 2016.
- [56] Q. Dou et al., "Automatic Detection of Cerebral Microbleeds From MR Images via 3D Convolutional Neural Networks," *IEEE Trans. Med. Imaging*, vol. 35, no. 5, pp. 1182–1195, 2016.
- [57] O. Maier, C. Schröder, N. D. Forkert, T. Martinetz, and H. Handels, "Classifiers for Ischemic Stroke Lesion Segmentation: A Comparison Study," *PLoS One*, vol. 10, no. 12, p. e0145118, Dec. 2015.
- [58] J. Cho, K. Lee, E. Shin, G. Choy, and S. Do, "How much data is needed to train a medical image deep learning system to achieve necessary high accuracy?," arXiv [cs.LG], 19-Nov-2015.
- [59] K. Lekadir et al., "A Convolutional Neural Network for Automatic Characterization of Plaque Composition in Carotid Ultrasound," *IEEE J Biomed Health Inform*, Nov. 2016.
- [60] J. Long, E. Shelhamer, and T. Darrell, "Fully convolutional networks for semantic segmentation," in *2015 IEEE Conference on Computer Vision and Pattern Recognition (CVPR)*, 2015.
- [61] J. Yosinski, J. Clune, Y. Bengio, and H. Lipson, "How transferable are features in deep neural networks?," in *Advances in Neural Information Processing Systems 27*, Z. Ghahramani, M. Welling, C. Cortes, N. D. Lawrence, and K. Q. Weinberger, Eds. Curran Associates, Inc., 2014, pp. 3320–3328.
- [62] H.-C. Shin et al., "Deep Convolutional Neural Networks for Computer-Aided Detection: CNN Architectures, Dataset Characteristics and Transfer Learning," *IEEE Trans. Med. Imaging*, vol. 35, no. 5, pp. 1285–1298, May 2016.
- [63] B. van Ginneken, A. A. A. Setio, C. Jacobs, and F. Ciompi, "Off-the-shelf convolutional neural network features for pulmonary nodule detection in computed tomography scans," in *2015 IEEE 12th International Symposium on Biomedical Imaging (ISBI)*, 2015.









Dear Editor,

We thank the anonymous reviewer for the positive response on our manuscript and the constructive comments. We have revised the manuscript accordingly, and in the following provide point-by-point responses to the comments and corresponding changes to the manuscript.

Sincerely,
Zeynettin Akkus, PhD

Comments to the author (if any):

Reviewer comments: This manuscript provides an overview of deep learning for quantitative brain MRI image analysis, specifically image segmentation. It is well structured and covers the major advances of deep learning in image segmentation studies for brain MRI.

A few minor things need to be addressed.

While the title of this paper is about quantitative analysis of brain MRI, it essentially focuses on the task of image segmentation. In order to better reflect the scope of this review, I would suggest changing the title to "deep learning for image segmentation on brain MRI" or something similar.

Answer: We changed the title to "Deep Learning for Brain MR Image Segmentation: State of The Art and Future Directions" as the reviewer suggested.

The mathematical description of dice similarity coefficient (DSC) is wrong, should be $DSC = 2 * TP / (2 * TP + FP + FN)$.

Answer: Thanks to the reviewer. We corrected this.

Please add references for cascaded CNN architecture on Page 8. Also, it would be helpful if the pros and cons of each architecture could be discussed here.

Answer: Thanks to the reviewer. We corrected this. We discussed pros and cons of each architecture in the discussion section. (Page 12)

Page 12 line 57, should the "pixel-wise architecture" be "patch-based architecture"?

Answer: Thanks to the reviewer. We corrected this.



Disclosure of potential conflicts of interest

Authors must disclose all relationships or interests that could have direct or potential influence or impart bias on the work. Although an author may not feel there is any conflict, disclosure of all relationships and interests provides a more complete and transparent process, leading to an accurate and objective assessment of the work. Awareness of a real or perceived conflicts of interest is a perspective to which the readers are entitled. This is not meant to imply that a financial relationship with an organization that sponsored the research or compensation received for consultancy work is inappropriate. For examples of potential conflicts of interests *that are directly or indirectly related to the research please visit:*

springer.com/gp/authors-editors/journal-author/journal-author-helpdesk/before-you-start

Journal of Digital Imaging

All authors of papers submitted to _____
(name of journal) must complete this form and disclose any real or perceived conflict of interest.

Please complete one form per author. The corresponding author collects the conflict of interest disclosure forms from all authors. The corresponding author will include a summary statement in the text of the manuscript in a separate section before the reference list, that reflects what is recorded in the potential conflict of interest disclosure form(s). Please note that you cannot save the form once completed. Kindly print upon completion, sign, and scan to keep a copy for your files.

The corresponding author should be prepared to send potential conflict of interest disclosure form if requested during peer review or after publication on behalf of all authors (if applicable).



I have no potential conflict of interest.

Category of disclosure	Description of Interest/Arrangement

Article title Deep learning for quantitative brain MRI: State of the art and future directions

Manuscript No. (if you know it) _____

Author name Zeynettin Akkus

Are you the corresponding author? Yes No

Herewith I confirm that the information provided is accurate.

Author signature  Date 03/15/2017

Deep Learning for Brain MRI Segmentation: State of The Art and Future Directions

Authors:

Zeynettin Akkus^{1*}, Alfiia Galimzianova^{2*}, Assaf Hoogi², Daniel L. Rubin², and Bradley J. Erickson^{1‡}

¹ Radiology Informatics Lab, Mayo Clinic, Rochester, MN, USA

² Department of Radiology, Stanford University School of Medicine, Stanford, CA, USA

* Both authors contributed equally to this work.

Abstract

Quantitative analysis of brain MRI is routine for many neurological diseases and conditions, and relies on accurate segmentation of structures of interest. Deep learning-based segmentation approaches for brain MRI are gaining interest due to their self-learning and generalization ability over large amounts of data. As the deep learning architectures are becoming more mature, they gradually outperform previous state-of-the-art classical machine learning algorithms. This review aims to provide an overview of current deep learning-based segmentation approaches for quantitative brain MRI. First we review the current deep learning architectures used for segmentation of anatomical brain structures and brain lesions. Next, the performance, speed, and properties of deep learning approaches are summarized and discussed. Finally, we provide a critical assessment of the current state, and identify likely future developments and trends.

Keywords: *Deep learning, quantitative brain MRI, convolutional neural network, brain lesion segmentation*

‡Corresponding Author: Bradley J. Erickson
200 First Street SW
Rochester, MN 55905
bje@mayo.edu

Acknowledgements:

This work was supported by National Institutes of Health 1U01CA160045, U01CA142555, 1U01CA190214, and 1U01CA187947.



Change of authorship request form

Please read the important information on page 4 before you begin

This form should be used by authors to request any change in authorship. Please fully complete all sections. Use black ink and block capitals and provide each author's full name with the given name first followed by the family name.

Section 1 Please provide the current title of manuscript

Manuscript ID no.JDIM-D-17-00060R1

Deep Learning for Brain MRI Segmentation: State of The Art and Future Directions

Section 2 Please provide the current authorship, in the order shown on your manuscript.

	First name(s)	Family name	ORCID or SCOPUS id, if available
1 st author			
2 nd author			
3 rd author			
4 th author			
5 th author			
6 th author			
7 th author			

Please use an additional sheet if there are more than 7 authors.

Section 3: Please provide a justification for change. Please use this section to explain your reasons for changing the authorship of your manuscript. Please refer to the journal policy pages for more information about authorship. Please explain why omitted authors were not originally included on the submitted manuscript.

Zeynettin originally submitted this with himself as corresponding author, but as he is a research fellow, he is not a 'permanent employee' and thus perhaps not the best person to serve as corresponding author, for purposes of readers that may wish to contact us.
In addition, the title was changed per a reviewer request.

Section 4 Proposed new authorship. Please provide your new authorship list in the order you would like it to appear on the manuscript.

	First name(s)	Family name (this name will appear in full on the final publication and will be searchable in various abstract and indexing databases)
1 st author		
2 nd author		
3 rd author		
4 th author		
5 th author		
6 th author		
7 th author		

Please use an additional sheet if there are more than 7 authors.

Section 5 Author contribution, Acknowledgement and Disclosures. Please use this section to provide revised Author Contribution, Acknowledgement and/or Disclosures of your manuscript, ensuring you state what contribution any new authors made and, if appropriate acknowledge any contributors who have been removed as authors. Please ensure these are updated in your manuscript.

New Disclosures (potential conflicts of interest, funding, acknowledgements):

New Author Contributions statement:

New Acknowledgement Section:

State 'Not applicable' if there are no new authors.

Change of authorship request form

Section 6 Declaration of agreement. **All** authors, unchanged, new and removed **must** sign this declaration.

* please delete as appropriate. Delete all of the bold if you were on the original authorship list and are remaining as an author

	First name	Family name		Signature	Affiliated institute	Date
1 st author			I agree to the proposed new authorship shown in section 4 /and the addition/removal* of my name to the authorship list.			
2 nd author			I agree to the proposed new authorship shown in section 4 /and the addition/removal* of my name to the authorship list.			
3 rd author			I agree to the proposed new authorship shown in section 4 /and the addition/removal* of my name to the authorship list.			
4 th authors			I agree to the proposed new authorship shown in section 4 /and the addition/removal* of my name to the authorship list.			
5 th author			I agree to the proposed new authorship shown in section 4 /and the addition/removal* of my name to the authorship list.			
6 th author			I agree to the proposed new authorship shown in section 4 /and the addition/removal* of my name to the authorship list.			
7 th author			I agree to the proposed new authorship shown in section 4 /and the addition/removal* of my name to the authorship list.			

Please use an additional sheet if there are more than 7 authors. * please delete as appropriate. Delete all of the bold if you were on the original authorship list and are remaining.

Important information. Please read.

- Please return this form, fully completed, to the editorial office. We will consider the information you have provided to decide whether to approve the proposed change in authorship. We may choose to contact your institution for more information or undertake a further investigation, if appropriate, before making a final decision.
- Please note, we cannot investigate or mediate any authorship disputes. If you are unable to obtain agreement from all authors (included those who you wish to be removed) you must refer the matter to your institution(s) for investigation. Please inform us if you need to do this.
- If you are not able to return a fully completed form within **30 days** of the date that it was sent to the author requesting the change, we may have to reject your manuscript. We cannot publish manuscripts where authorship has not been agreed by all authors (including those who have been removed).
- Incomplete forms will be rejected.